

PMSTPCOL PEmails

From: Govan, Tekia
Sent: Monday, September 21, 2009 11:20 AM
To: STPCOL
Subject: FW: Responses to Requests for Additional Information
Attachments: U7-C-STP-NRC-0900134 R01.pdf

Tekia V. Govan, Project Manager
U.S. Nuclear Regulatory Commission
Office of New Reactors
MS T-7-F29
Washington DC 20555-0001
301-415-6197
Tekia.Govan@nrc.gov

From: Ballinger, Amy [mailto:aballinger@STPEGS.COM]
Sent: Wednesday, September 16, 2009 5:56 PM
To: Muniz, Adrian; Sosa, Belkys; Dyer, Linda; Wunder, George; Eudy, Michael; Plisco, Loren; Anand, Raj; Foster, Rocky; Joseph, Stacy; Govan, Tekia; Tai, Tom
Subject: Responses to Requests for Additional Information

Good Afternoon,

Attached, please find a courtesy copy of the letter sent to the NRC in response to the request for additional information related to COLA Part 2, Tier 2, Chapter 2. If you have any questions, contact Dick Bense at 361-972-4802

Amy Ballinger
STP Units 3 & 4
Licensing Specialist
Phone: (361)972-4644
Fax: (361) 972-4751

Hearing Identifier: SouthTexas34Public_EX
Email Number: 1759

Mail Envelope Properties (83F82891AF9D774FBBB39974B6CB134F94B6BAE88B)

Subject: FW: Responses to Requests for Additional Information
Sent Date: 9/21/2009 11:19:46 AM
Received Date: 9/21/2009 11:19:47 AM
From: Govan, Tekia

Created By: Tekia.Govan@nrc.gov

Recipients:
"STPCOL" <STP.COL@nrc.gov>
Tracking Status: None

Post Office: HQCLSTR01.nrc.gov

Files	Size	Date & Time
MESSAGE	921	9/21/2009 11:19:47 AM
U7-C-STP-NRC-0900134 R01.pdf		1367722

Options
Priority: Standard
Return Notification: No
Reply Requested: No
Sensitivity: Normal
Expiration Date:
Recipients Received:



South Texas Project Electric Generating Station P.O. Box 289 Wadsworth, Texas 77483

September 16, 2009
U7-C-STP-NRC-090134

U. S. Nuclear Regulatory Commission
Attention: Document Control Desk
One White Flint North
11555 Rockville Pike
Rockville, MD 20852-2738

South Texas Project
Units 3 and 4
Docket Nos. 52-012 and 52-013
Responses to Requests for Additional Information

Attached are responses to NRC staff questions in Request for Additional Information (RAI) letter number 185, related to COLA Part 2, Tier 2, Sections 2.4S.5, "Probable Maximum Surge and Seiche Flooding," 2.4S.6, "Probable Maximum Tsunami Hazards," and 2.4S.13, "Accidental Releases of Radioactive Liquid Effluents in Ground and Surface Waters."

This letter includes the complete response to RAI letter number 185. Attachments 1 through 7 provide the responses to the following NRC staff questions included in RAI letter number 185:

02.04.05-8	02.04.06-4	02.04.13-11	02.04.13-13
02.04.05-9		02.04.13-12	02.04.13-14

When a change to the COLA is indicated, the change will be incorporated into the next routine revision of the COLA.

There are no commitments in this letter.

If you have any questions regarding these responses, please contact me at (361) 972-7206, or Bill Mookhoek at (361) 972-7274.

I declare under penalty of perjury that the foregoing is true and correct.

Executed on 9/16/2009



Mark A. McBurnett
Vice President, Oversight and Regulatory Affairs
South Texas Project Units 3 & 4

rhb

Attachments:

1. RAI 02.04.05-8
2. RAI 02.04.05-9
3. RAI 02.04.06-4
4. RAI 02.04.13-11
5. RAI 02.04.13-12
6. RAI 02.04.13-13
7. RAI 02.04.13-14

cc: w/o attachments and enclosure except*
(paper copy)

(electronic copy)

Director, Office of New Reactors
U. S. Nuclear Regulatory Commission
One White Flint North
11555 Rockville Pike
Rockville, MD 20852-2738

*George Wunder
*Tekia Govan

Loren R. Plisco
U. S. Nuclear Regulatory Commission

Regional Administrator, Region IV
U. S. Nuclear Regulatory Commission
611 Ryan Plaza Drive, Suite 400
Arlington, Texas 76011-8064

Steve Winn
Eddy Daniels
Joseph Kiwak
Nuclear Innovation North America

Kathy C. Perkins, RN, MBA
Assistant Commissioner
Division for Regulatory Services
Texas Department of State Health Services
P. O. Box 149347
Austin, Texas 78714-9347

Jon C. Wood, Esquire
Cox Smith Matthews

J. J. Nesrsta
R. K. Temple
Kevin Pollo
L. D. Blaylock
CPS Energy

Alice Hamilton Rogers, P.E.
Inspection Unit Manager
Texas Department of State Health Services
P. O. Box 149347
Austin, Texas 78714-9347

C. M. Canady
City of Austin
Electric Utility Department
721 Barton Springs Road
Austin, TX 78704

*Steven P. Frantz, Esquire
A. H. Gutterman, Esquire
Morgan, Lewis & Bockius LLP
1111 Pennsylvania Ave. NW
Washington D.C. 20004

*George F. Wunder
*Tekia Govan
Two White Flint North
11545 Rockville Pike
Rockville, MD 20852

RAI 02.04.05-8**Question:**

The applicant responded to RAI 02.04.05-3 in a letter dated August 27, 2008. The staff determined that the justification for not performing a PMH backwater calculation for the Little Robbins Slough should be included in the FSAR. Provide proposed text changes for FSAR Section 2.4.5 that address this issue.

Response:

The first paragraph of Subsection 2.4S.5.2.3.2 of STP COLA FSAR, Revision 3, which will be submitted in September, 2009, will be revised to include the justification provided in the response to RAI 02.04.05-3 for not performing a PMH backwater calculation for the Little Robbins Slough:

“A modified version of the Halff HEC-RAS hydraulic model (i.e., Reference 2.4S.5-10) was used to estimate the water surface elevation at STP 3 & 4 based on a backwater calculation on the Colorado River using the storm surge water surface elevation near the open coast as the downstream boundary condition. The Halff HEC-RAS model was developed for Halff’s flood damage evaluation study and is discussed extensively in Subsection 2.4S.3. To be on the conservative side, however, the floodplain-extension used in HEC-RAS model of Subsection 2.4S.3 was not adopted in estimating the storm surge at STP 3 & 4. Little Robbins Slough near the STP site, shown in Figure 2.4S.5-XX, is a shallow multi-channel slough that joins Robbins Slough, a brackish marsh, which eventually drains to the Gulf Intracoastal Waterway. With the PMSS, it would be completely submerged and drowned out, thereby resulting in negligible water surface slopes for the backwater calculation. Therefore, the Colorado River is used for the PMSS backwater calculation in order to generate a bounding PMSS water level at STP 3 & 4.”

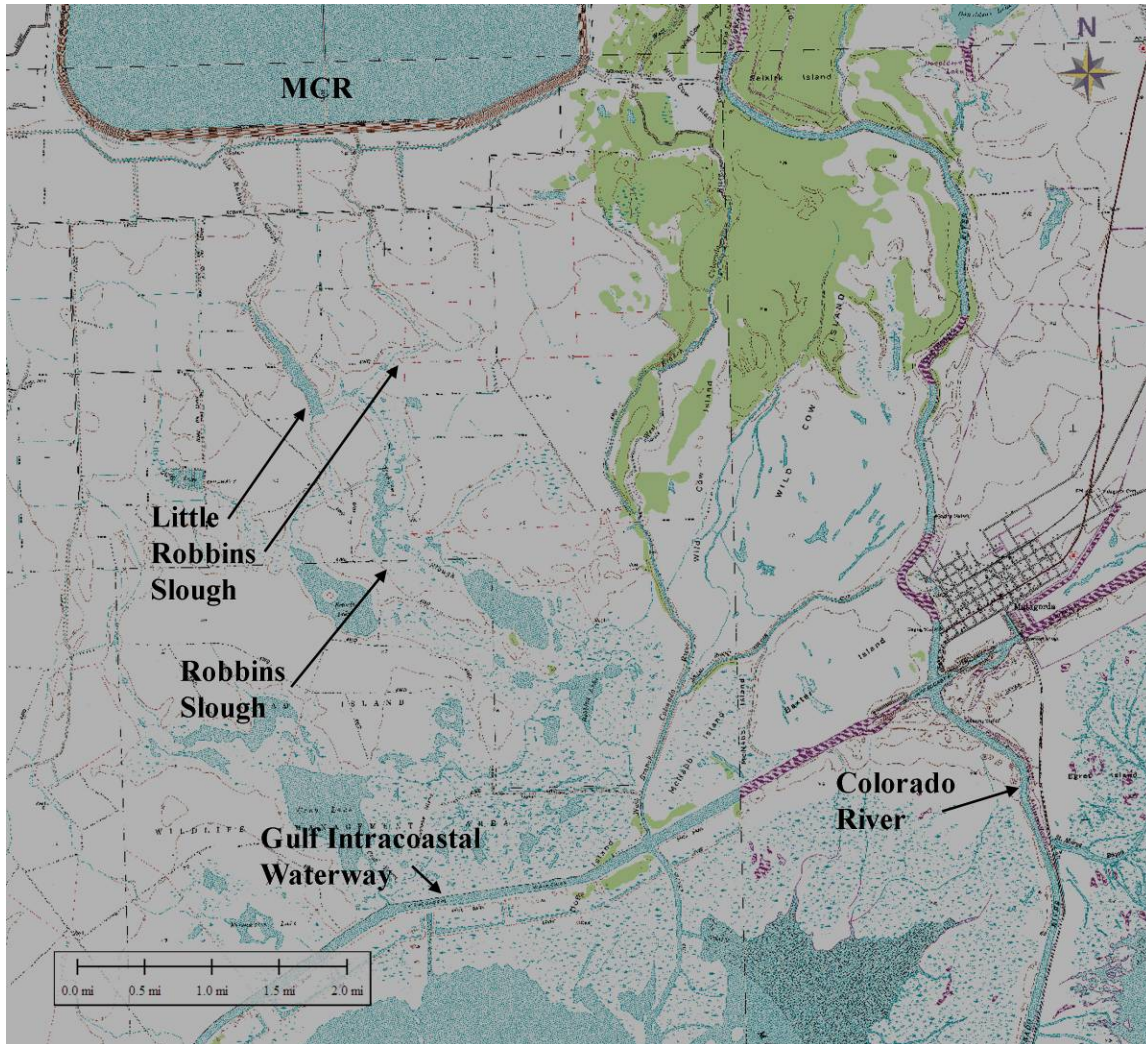


Figure 2.4S.5-XX. USGS Quadrangle showing Little Robbins Slough and Colorado River relative to the STP 3 & 4 Main Cooling Reservoir (MCR).

RAI 02.04.05-9**Question:**

The extrapolation procedure used to estimate the Maximum of Maximum Envelope of Water (MOM) surface elevation corresponding to the Probable Maximum Hurricane (PMH) in the RAI response is not adequately explained, nor provide any technical basis for the relationship between the Maximum of Maximum Envelope of Water surface elevations and the ΔP for hurricanes of categories 1-5. The fact that extrapolated Maximum of Maximum Envelope of Water surface elevation from this relationship is greater than the estimated water surface elevation from the SURGE model, the applicant needs to provide a sufficient basis for characterizing it as being conservative.

Provide one of the following: (a) a physical basis to justify why the Maximum of Maximum Envelope of Water surface elevation- ΔP relationship is valid, (b) citation to an accepted and validated method that uses such a relationship, or (c) justification with citation why estimating parameters of a third-degree polynomial relationship from five data points would result in an accurate estimation of the model parameter values. Alternatively, provide an analysis that uses a model consistent with the available data.

Response:

FSAR 2.4S.5.2, "Surge and Seiche Water Levels," provides the descriptions and analysis necessary to demonstrate that the STP site is adequately protected from flooding due to the probable maximum storm surge (PMSS) resulting from the probable maximum hurricane (PMH). The discussion and analysis provided in FSAR 2.4S.5.2 conforms to Standard Review Plan 2.4.5, "Probable Maximum Surge and Seiche Flooding," that the "storm surge induced by the PMH should be estimated as recommended by Regulatory Guide 1.59, supplemented by current best practices."

As described in FSAR 2.4S.5.2.2, two different methods were used to estimate the probable maximum storm surge (PMSS) at STP 3 & 4. The first method used the computer program, "Quasi Two-Dimensional Open Coast Storm Surge," known as SURGE, to estimate the PMSS water surface elevation at the coast near Matagorda, Texas. A calibrated model developed by Halff Associates (i.e., the Halff HEC-RAS model described in FSAR Section 2.4S.3) is then used to estimate the resulting PMSS water surface elevation at the STP 3 & 4 site. The second method used the results from NOAA's model, "Sea, Lake, and Overland Surges from Hurricanes" (SLOSH) to estimate the PMSS water surface elevation at the STP 3 & 4 site. A third method, i.e., the method prescribed in Revision 2 of Regulatory Guide 1.59, dated August 1977, was used to estimate PMSS in order to demonstrate conformance with guidance provided in SRP 2.4.5. As described in FSAR 2.4S.5.2.5, this method is no longer considered valid and was not used to demonstrate that ABWR DCD limits for storm surge are met.

Either of the two methods presented in FSAR 2.4S.5.2 (SURGE or SLOSH), will satisfy requirements to demonstrate that the STP 3 & 4 site is adequately protected from PMSS resulting from the PMS, notwithstanding the fact that estimates of PMSS based on the SURGE model are significantly lower than the estimates of PMSS based on the SLOSH model. This position is

consistent with NUREG-0933, "A Prioritization of Generic Safety Issues - Item C-14: Storm Surge Model for Coastal Sites (Rev. 1)," dated 2007. NUREG-0933, Item C-14, which evaluated the use of SURGE, "a 'bathystrophic' model developed by the U.S. Army Corps of Engineers, Coastal Engineering Research Center (CERC)," against newer multidimensional dynamic mathematical models such as SLOSH. Following this evaluation, NUREG-0933, Item C-14, provided the following conclusion:

The staff believes that the existing bathystrophic model (SURGE) is adequate for calculating design basis water levels at future nuclear plant sites. This model is very conservative and is still used by the CERC. Its use is specified in SRP Section 2.4.5-3. Furthermore, as stated in the SRP, the use of other verified modes is not precluded. Thus, this licensing issue does not require any changes to be made by the staff and it is recommended it be dropped from further consideration.

This RAI is a follow-up to the response to RAI 02.04.05-4 (Letter ABR-AE-08000072, dated September 10, 2008 (ML082550125), which requested that STPNOC describe and then justify the method used to extrapolate the results of the SLOSH model beyond a Category 5 hurricane. In response to the request to describe the extrapolation method, RAI 02.04.05-4 explained that a least-squares curve fit, based on a third-degree polynomial relationship, was used to extrapolate SLOSH results and extensive details were provided. In response to the request "How was it verified that the extrapolation was valid and conservative?," RAI 02.04.05-4 explained:

...validation of the extrapolation requires testing the results against another, more conservative method. As stated in Rev 0 of Subsection 2.4S.5.2.4, "the PMSS at STP 3 & 4 predicted by SLOSH, with the sea level adjustments, is 31.1 feet MSL. This value is more conservative than the SURGE estimate of 24.29 feet MSL at STP 3 & 4." For coastal locations, the SURGE model is considered conservative as discussed in NUREG-0933.

STPNOC acknowledges that the term "more" in the phrase "against another, more conservative method" is inaccurate. However, the intent of this response is clear. SLOSH results, which include results based on the extrapolation method being challenged, are more conservative than the results independently calculated using the SURGE method. Because SURGE results are considered conservative based on the conclusions in NUREG-0933, Item C-14, the SLOSH results, which include results based on the extrapolation, are also conservative.

The second paragraph of this RAI presents three options for justifying STPNOC's use of a third-degree polynomial relationship to extrapolate the results of the SLOSH model. The justification described above provides a comprehensive justification that eliminates the need to address any or all of the methods for justification suggested in the RAI.

STPNOC is cognizant that the objective of FSAR 2.4S.5.2 is to demonstrate that the STP site is adequately protected from flooding due to the probable maximum storm surge (PMSS) resulting from the probable maximum hurricane (PMH). The acceptance criteria for the probable maximum surge and seiche flooding is in ABWR DCD, Table 2.1-1, Limits Imposed on SRP

Section II Acceptance Criteria by ABWR Design, which establishes a limit of 30.5 cm (1 foot) below grade for the probable maximum surge and seiche flooding. The nominal plant grade for STP 3 & 4 is 34 feet above mean sea level (MSL). As stated in FSAR 2.4S.5.2.4, the PMSS at STP 3 & 4 is 31.1 feet MSL when estimated by the SLOSH model. As stated in FSAR 2.4S.5.2.3.2, the PMSS at STP 3 & 4 is 24.29 feet MSL when independently estimated by the SURGE model. Therefore, FSAR 2.4S.5.2 demonstrates, using two independent methods, that the requirements in ABWR DCD, Table 2.1-1 are met.

Additionally, Revision 3 of FSAR 2.4S.2.2, "Flood Design Considerations," which will be submitted in September of 2009, explains that all STP 3 & 4 power block safety-related structures are designed to prevent any flooding of safety-related SSCs for water levels below the design basis flood elevation of 40.0 ft MSL. This requirement was established to address a Main Cooling Reservoir breach, which is the design basis flood for STP 3 & 4. As a result, STP 3 & 4 is protected against the probable maximum surge and seiche flooding well above the limit required by ABWR DCD, Table 2.1-1 (i.e., 40.0 ft MSL versus 30.5 cm (1 foot) below 34 foot MSL grade).

Based on all of the above, FSAR 2.4S.5.2 demonstrates STP 3 & 4 is protected against the PMSS resulting from the PMH, including appropriate consideration of the most severe natural phenomena historically reported for the site and surrounding area, with sufficient margin for the limited accuracy, quantity, and time period in which the historical data have been accumulated.

No COLA revision is required as a result of this response.

RAI 02.04.06-4**Question:**

In the review by the staff of the response to RAI 02.04.06-1 (U7-C-STP-NRC-080067, December 4, 2008), the staff has generated the following additional questions: (1) It appears that the applicant's maximum tsunami water levels are not runup levels (including overland flow) but shoreline water surface elevations; (2) The applicant does not provide sufficient justification to dismiss the possibility that the Campeche Escarpment is a potential source for the PMT water levels; and (3) The applicant discusses the finding that no evidence of tsunami deposits was found near the site and that potential tsunami deposits from the East Breaks source would have been emplaced during sea-level low stand. However, they do not mention older tsunami deposits that occur during sea-level high stands, such as the Falls County tsunami deposit (Bourgeois and others, 1988). The applicant should clarify these issues and provide proposed text changes for FSAR Sections 2.4S.6.

Response:

With respect to Item (1), the Method of Splitting Tsunami (MOST) hydrodynamic code includes three phases of tsunami evolution (Reference 1):

- (i) A “Deformation Phase” that generates the initial conditions for a tsunami by simulating ocean floor and corresponding free surface changes due to a forcing mechanism;
- (ii) A “Propagation Phase” that propagates the generated tsunami across the deep ocean using Nonlinear Shallow Water (NSW) wave equations; and
- (iii) An “Inundation Phase” that simulates the shallow ocean behavior of a tsunami by extending the NSW calculations using a multi-grid runup algorithm to predict coastal flooding and inundation.

The maximum tsunami water levels presented in the response to RAI 02.04.06-1 were based on simulation results of the inundation phase of MOST. The inundation phase includes estimates of runup elevations onto land. Details of the moving boundary calculation for the inundation phase are discussed in Reference 2. A discussion of the MOST code is provided in STP COLA Revision 3, Subsection 2.4S.6, scheduled for submittal to the NRC in September 2009.

With respect to Item (2), the Campeche Escarpment is located approximately 873 km (542 mi) from the STP 3 & 4 site. The Campeche Escarpment is much further away from the STP 3 & 4 site than the East Breaks slump, which is located about 142 km (88 mi) from the STP 3 & 4 site. Locations of the Campeche Escarpment and the East Breaks slump are shown in Figure 1 of this response. It is explained in the response to RAI 02.04.06-1 that tsunamis generated from submarine mass failures (SMFs) from remote areas of the Gulf of Mexico, such as the Campeche Escarpment, are not expected to exceed the four initial conditions simulated for the East Breaks slump. Maximum wave heights and minimum wave heights for the four simulated initial conditions are listed in Table 1.

With respect to assessing potential SMF dimensions for the Campeche Escarpment, little data is available. For example, Reference 3 states that “presently, there is no published information

showing the detailed bathymetry, nor distribution of landslides on or above the Campeche Escarpment.” However, Reference 3 states the following general information with respect to the carbonate province, which includes the Campeche Escarpment:

“the carbonate platform edge that is exposed along the southern part of the Florida Escarpment and the Campeche Escarpment has been eroded since its initial formation and lagoonal facies are now exposed on the cliff face. The present morphology of these sections of the escarpments is quite different from the northern part of the Florida Escarpment. Here canyons with steep sides and near-vertical headwalls, called box canyons, incise these parts of the escarpments. These box canyons may be the result of dissolution of the limestone by discharge of acidic groundwater at the base of the escarpment in the canyon heads that resulted in collapse of the steep canyon headwalls. A large talus deposit has been identified in seismic profiles along the base of the Campeche Escarpment that was deposited prior to the mid-Cretaceous. The full extent of this deposit is unknown because of limited seismic coverage. Breccia recovered from a DSDP [Deep Sea Drilling Program] hole near the base of the Campeche Escarpment presumably is the result of topples and falls from the escarpment face. The amount of material associated with an individual failure is unknown. Talus blocks up to 5-m across and rubble have been observed on the seafloor along the base of the southern part of the Florida Escarpment which suggests this cliff has recently undergone erosion. The talus deposits in the heads of some of the box canyons cover areas less than 15 km², and their thickness is unknown. Published information suggests that the recent falls and topples were limited to the southern part of the Florida Escarpment and perhaps the Campeche Escarpment, but those that have been mapped are of limited aerial extent and are concentrated in the heads of box canyons.”

Source parameters for the Campeche Escarpment postulated in Reference 3 do not exceed the source parameters that were simulated for the East Breaks slump in RAI 02.04.06-1. In addition, as tsunamis generated from landslides tend to be steep (i.e., high initial wave height relative to wavelength) and are prone to breaking, a tsunami event from a SMF in the Campeche Escarpment is not expected to propagate across the Gulf of Mexico and sustain wave heights that exceed the four simulated initial conditions for the East Breaks slump. As shown with the model simulations for the East Breaks slump, significant diffusion and energy dissipation of large initial waves occurs due to the continental shelf that extends offshore of the South Texas coast. Therefore, runup along the South Texas coast from a Campeche Escarpment event is likely to be negligible.

Information relative to the tsunami modeling simulations is provided in STP COLA Revision 3, Subsection 2.4S.6, scheduled for submittal to the NRC in September 2009.

Table 1. Initial wave deformation characteristics and maximum runup for simulations.

Case	Initial Wave Deformation Area	Minimum Initial Wave Height relative to NGVD 29	Maximum Initial Wave Height above NGVD 29	Maximum Runup above NGVD 29
	(sq. km)	(m)	(m)	(m)
PV	411	-7	3	1
PV(x20)	387	-140	60	2
PNG	879	-20	16	2
Monster	9932	-38	27	2

[Modified from Table 1 of the response to RAI 02.04.06-1]

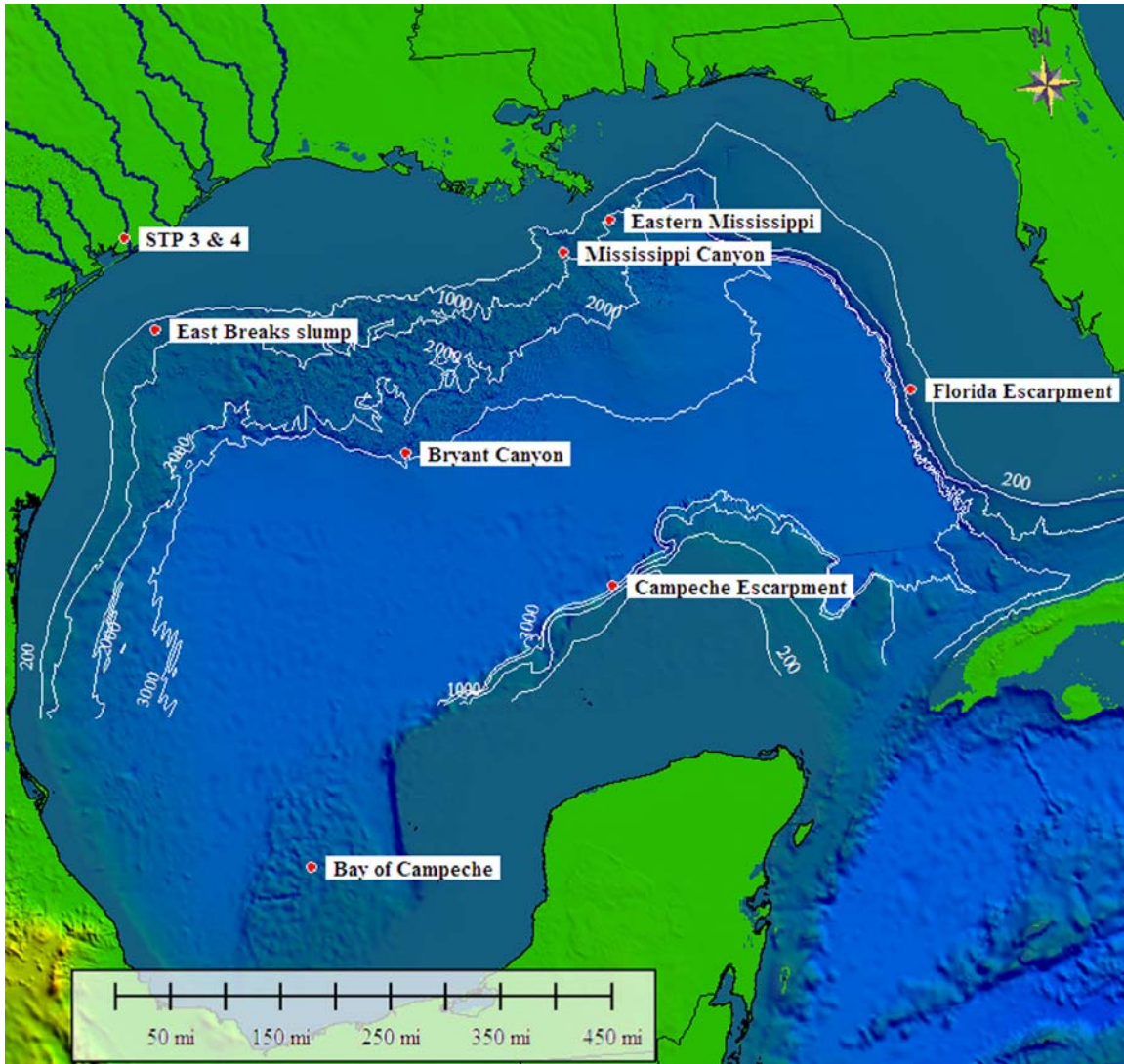


Figure 1. Submarine Mass Failure (SMF) regions in the Gulf of Mexico (Reference 3). Gulf of Mexico depth contours shown in meters below present-day sea level (Source: Reference 4).

With respect to Item (3), the event deposits occurring in Falls County, Texas, and interpreted by some investigators as tsunamigenic are not discussed in the response to RAI 02.04.06-1 (U7-C-STP-NRC-080067, December 4, 2008) for the following reasons:

The event deposits occurring in Falls County that are discussed in Bourgeois et al. (1988) (Reference 5) are located about 167 mi to the north-northwest of the STP 3 & 4 site and about 175 mi from the South Texas coast (Figure 2). In Bourgeois et al. (1988) (Reference 5), the source of the deposits is cited as a large diameter (>10 km) extraterrestrial bolide that impacted the Earth about 65.5 million years ago (hereinafter referred to as the “Chicxulub impact”). The Chicxulub impact occurred at or near the Cretaceous–Paleogene boundary (K/P), which historically and for this response, is also referred to as the Cretaceous-Tertiary (K/T) boundary (Reference 5). The approximate location of Chicxulub impact is shown in Figure 2 (Reference 6).

With respect to the sea-level high stand in the Late Maastrichtian (65.5 to 68.5 million years ago), Reference 7 estimates that the global sea level was approximately 150 m to 250 m (492 ft to 820 ft) higher than the present-day sea level. The paleo-shoreline for North America during the Late Maastrichtian is presented in Figure 2 (Reference 8 and Reference 9).

The origin of a potential tsunami deposit at the Falls County site and whether it coincides with the K/T boundary has been debated in the scientific literature (Reference 10). Bourgeois et al. (1988) (Reference 5) stated that “at sites near the Brazos River, Texas, an iridium anomaly and the Cretaceous-Tertiary [K/T] boundary directly overlie a sandstone bed in which coarse-grained sandstone with large clasts of mudstone and reworked carbonate nodules grades upward to wave ripple-laminated, very fine grained sandstone. This bed is the only sandstone bed in a sequence of uppermost Cretaceous to lowermost Paleocene mudstone that records about 1 million years of quiet water deposition in midshelf to outer shelf depths. Conditions for depositing such a sandstone layer at these depths are most consistent with the occurrence of a tsunami about 50 to 100 meters high. The most likely source for such a tsunami at the Cretaceous-Tertiary boundary is a bolide water impact.”

Gale (2006) (Reference 6) stated that “Bourgeois et al. (1988) (Reference 5), [and others] interpreted the erosional surface to have been created by a huge tsunami wave generated by the terminal Cretaceous bolide impact at Chicxulub in the Yucatan Peninsula of Mexico [Figure 2]. However, the presence of burrows in the top Corsciana Clay and borings in the reworked concretions incorporated in the overlying conglomerate indicate that formation of the erosional surface was followed by a long period of non-deposition, not by deposition of tsunami transported sediment. A plausible alternative explanation is that the erosional surface formed as a result of sea-level fall and is therefore the highest sequence boundary in the Cretaceous. The channels have a NE-SW orientation and a depth of 1-2 m and were probably formed by bottom currents running approximately at right angles to the palaeocoast.”

Shulte et al. (2005) (Reference 9) concluded that the event deposits coincided with the K/T boundary but stated that “the high variability of storm- and tsunami-related event deposits makes it difficult to point out characteristics for either depositional mechanism.” Similarly, Keller et al.

(2004) (Reference 10) interpreted the sedimentology and paleontology of the event deposits to indicate that a tsunami backflow interpretation is not supported by the data from outcrops and cores in Texas or northeastern New Mexico.

Based on the uncertainty regarding the nature of the Falls County deposits, whether they are paleotsunami deposits, deposits from high-energy storm events, or related to sea-level fall in the Late Maastrichtian, they are not considered in the evaluation of relevant tsunamigenic sources for STP 3 & 4. In addition, Regulatory Guide 1.206, NUREG-0800, and NUREG/CR-6966 (Reference 11) do not identify low-probability bolide impacts as a credible generator of tsunamis within the operating life of a nuclear power plant.

No further COLA revision is required as a result of this RAI response.

RAI 02.04.13-11**Question:**

In its review of the applicant's response to RAI 02.04.13-6, the staff noted that the applicant, STP, proposed revisions to the FSAR that state "the minimum laboratory K_d values (or the 10th percentile of the data distribution provided in Reference 2.4S.13-9...)", and "the maximum laboratory K_d values (the 10th percentile of the data distribution provided in Reference 2.4S.13-9...)". These two statements appear to identify the same 10th percentile value to represent the minimum and maximum. Staff requests the applicant clarify their proposed change to the FSAR. In addition, staff request that the applicant provide a technical justification for selecting the 10th percentile (and perhaps 90th percentile) values rather than the minimum and maximum in the conservative analysis to be completed.

Response:

The minimum and maximum of the site-specific laboratory-determined K_d values for each radionuclide of concern, which were used to complete a transport sensitivity analysis, are described in FSAR Section 2.4S.13.1.4. For those radionuclides for which a site-specific K_d value was not determined, the 10th and 90th percentiles of the lognormal K_d probability distributions from Reference 1 were used in the sensitivity analysis to represent the minimum and maximum K_d values, respectively. These percentiles are the lower and upper bounds, respectively, of the 80- percent confidence interval for a lognormal probability distribution. That is to say, there is a 10-percent probability that a value in the distribution is less than the 10th percentile and a 10-percent probability that a value in the distribution is greater than the 90th percentile.

A comparison of the minimum laboratory-measured site-specific K_d values with the corresponding 10th percentile K_d values of the probability distributions from Reference 1 reveals that for Cs and Pu the 10th percentile values from Reference 1 are about half the site-specific minimum values, while the 10th percentile K_d values from Reference 1 for Ni and Sr are about twice the corresponding site-specific minimum K_d values. The 90th percentiles of the probability distributions from Reference 1 are substantially greater than the site-specific maximum K_d values for all of the radionuclides of concern.

To apply an additional measure of conservatism, the sensitivity analysis was repeated using the 2.3th and 97.7th percentiles of the K_d data distributions to represent the minima and maxima, respectively, of the distributions for those radionuclides for which no site-specific K_d values were determined. These values are two standard deviations from the mean of a lognormal cumulative probability distribution and determine the lower and upper bounds, respectively, of the 95-percent confidence interval for the distribution. The 95-percent confidence interval is a commonly used statistical measure for determining an acceptable level of uncertainty. The lower and upper bounds of this interval establish those values for which the probability of a member of the distribution being less than or greater than the value, respectively, is 2.3 percent. The sensitivity analysis described in FSAR Section 2.4S.13.1.4 was repeated, using the 2.3th and 97.7th percentiles of the probability distribution for yttrium/scandium from Reference 1 instead of the 10th and 90th percentiles to represent the minimum and maximum K_d values, respectively,

for Y. The results of the sensitivity analysis were the same when the lower minimum K_d and the higher maximum K_d values were substituted for the 10th and 90th percentiles.

The second and third paragraphs of COLA Rev. 03, Section 2.4S.13.1.4 will be revised as follows:

A sensitivity analysis was performed using the range of average linear velocities/travel times from Table 2.4S.12-17 and the range of distribution coefficients (K_d) from Table 2.4S.13-3. For example, the maximum average linear velocity (shortest travel time) incorporated the minimum laboratory site-specific K_d values (or the 10th percentile of the data distribution provided Reference 2.4S.13-9 or the 2.3th percentile of the data distribution provided in Reference 2.4S.13-10 for those isotopes without site specific laboratory tests) and the minimum average linear velocity (longest travel time) incorporated the maximum laboratory site-specific K_d values (or the 10th percentile of the data distribution provided Reference 2.4S.13-9 or the 97.7th percentile of the data distribution provided in Reference 2.4S.13-10 for those isotopes without site specific laboratory tests).

The result of the sensitivity analysis indicates that only the predicted tritium concentration (1.08 E-03 $\mu\text{Ci/cc}$) for Transport Pathway 1a would slightly exceed its ECL (1.00 E-03 $\mu\text{Ci/cc}$) when using the maximum average linear velocity (minimum travel time) and minimum K_d laboratory values (or the 2.3th percentile of the data distribution provided in Reference 2.4S.13-10 for yttrium/scandium) for Transport Pathway 1a. The geologic depositional environment at the STP site suggests that the use of the maximum average linear velocity would be extreme and that the representative average linear velocities used in the analyses best represent the hydrogeologic conditions beneath the STP site. The representative average linear velocities derived utilizing averages and geometric means of the material properties would best represent the discontinuous, fine-grained mixtures of the sand, silt, and clay subsurface materials described in Subsection 2.4S.12. Using the representative average linear velocities, no radionuclides are predicted to exceed their respective ECLs.

The attached addition to Table 2.4S.13-3, "Laboratory Distribution Coefficient Measurements in mL/g for the Upper Shallow Aquifer" will be added as Sheet 2 of 2 to Table 2.4S.13-3.

Reference:

1. "Development of Probabilistic RESRAD 6.0 and RESRAD-BUILD 3.0 Computer Codes," NUREG/CR-6697, Yu, C., LePoire, D., Gnanapragasam, E., Arnish, J., Kamboj, S., Biwer, B.M., Cheng, J-J, Zilen, A., and Chen, S.Y., Argonne National Laboratory, 2000.

Table 2.4S-13.3 (continued) Laboratory Distribution Coefficient Measurements in mL/g for the Upper Shallow Aquifer

Boring Id	Sample Id	Corresponding Well	Replicate Analysis	Fe K _α		Ni K _α		Pu K _α		Co K _α		Sr K _α		Cs K _α		
				Value	Ave.	St Dev	Value	Ave.	St Dev	Value	Ave.	St Dev	Value	Ave.	St Dev	Value
B-308	SS15 ⁽¹⁾	OW-308 U	-	>2079.1	1675.9	-	29.8	-	242.8	34.3	13.5	2.1	0.4	-	359.9	12.7
			1	>3264.1	-	33.1	-	218.5	-	14.2	-	2.3	-	368.9	-	-
			2	>384.1	-	26.5	-	267.0	-	12.8	-	1.8	-	351.0	-	-
B-332	SS12	OW-332 U	-	45.4	22.7	224.4	192.4	52.7	65.3	17.8	6.4	1.5	0.1	59.5	61.0	2.2
			1	29.3	-	88.3	-	77.9	-	6.7	-	1.4	-	62.6	-	-
			2	61.4	-	360.4	-	-	-	6.2	-	1.6	-	-	-	-
B-348	SS8	OW-348 U	-	>2021.8	1517.9	23.0	0.5	110.8	102.3	12.0	10.9	2.0	0.4	433.1	348.1	120.1
			1	>948.5	-	23.4	-	93.8	-	11.0	-	1.7	-	263.2	-	-
			2	>3095.1	-	22.7	-	109.2	-	10.9	-	2.4	-	147.4	-	50.1
B-349	SS14	OW-349 U	-	98.8	48.6	233.9	43.2	118.3	109.2	12.9	7.7	1.0	0.7	182.8	147.4	50.1
			1	65.4	-	264.4	-	100.1	-	9.5	-	1.5	-	112.0	-	-
			2	134.2	-	203.4	-	-	-	6.0	-	0.6	-	-	-	-
B-408	SS14	OW-408 U	-	>3308.4	3471.7	26.8	0.6	55.4	55.4	5.6	15.2	3.1	1.6	197.7	189.1	12.2
			1	>5763.3	-	27.2	-	59.3	-	16.7	-	4.3	-	197.7	-	-
			2	>853.6	-	26.4	-	51.4	-	13.8	-	2.0	-	180.5	-	-
B-438	SS12	OW-438 U	-	>751.9	219.1	20.0	1.7	180.2	180.2	3.2	12.8	1.7	0.5	321.0	321.0	19.3
			1	>906.8	-	18.8	-	177.9	-	14.1	-	2.1	-	334.6	-	-
			2	>597.0	-	21.2	-	182.5	-	11.5	-	1.4	-	307.4	-	-
B-910	SS14	OW-910 U	-	289.7	304.7	110.7	85.7	364.5	364.5	316.4	10.3	1.7	0.4	212.1	212.1	8.7
			1	74.3	-	171.3	-	140.7	-	9.9	-	1.3	-	206.0	-	-
			2	505.2	-	50.1	-	598.2	-	10.6	-	2.0	-	218.3	-	-
B-930	SS14	OW-930 U	-	>952.0	697.4	31.0	7.1	1060.8	1060.8	357.4	11.2	3.1	0.7	554.5	554.5	10.3
			1	>458.9	-	28.1	-	808.1	-	12.1	-	3.5	-	561.8	-	-
			2	>1445.2	-	36.0	-	1313.5	-	10.3	-	2.6	-	547.2	-	-
B-933	SS14	OW-933 U	-	>1780.5	1266.0	25.2	1.7	53.6	53.6	10.5	14.9	3.0	0.2	486.2	486.2	38.4
			1	>885.3	-	24.0	-	61.1	-	14.3	-	2.9	-	513.3	-	-
			2	>2875.7	-	26.4	-	46.2	-	15.5	-	3.1	-	459.0	-	-
B-934	SS15	OW-934 U	-	>3361.0	3275.5	27.9	0.5	447.5	447.5	247.8	6.3	1.6	0.3	113.1	113.1	8.2
			1	>5677.1	-	27.5	-	302.3	-	6.3	-	1.3	-	119.0	-	-
			2	1044.9	-	28.2	-	652.8	-	6.4	-	1.8	-	107.3	-	-
Summary Statistics																
Number of samples																
Minimum																
Maximum																
Arithmetic Mean																
Geometric Mean																
Standard Deviation																
Skewness																
				Fe K _α	Ni K _α	Pu K _α	Co K _α	Sr K _α	Cs K _α							
				10.0	10.0	10.0	10.0	10.0	10.0							
				45.4	20.0	53.6	6.3	1.0	61.0							
				>3361.0	233.9	1060.8	15.2	3.1	554.5							
				>1469.0	75.3	268.2	10.9	2.1	279.2							
				>775.0	46.4	166.5	10.4	2.0	231.5							
				>1238.8	85.4	309.7	3.3	0.7	162.2							
				>0.4	1.5	2.2	-0.2	0.4	0.4							

Note: (1) Broken jar sample. Contents transferred to secondary jar prior to shipment to laboratory.

RAI 02.04.13-12**Question:**

In the review by staff of the K_d report provided in response to RAI 02.04.13-7, staff has generated the following requests:

(A) (1) comment on the creation of a secondary stock solution - it is not mentioned or defined in methodology, (2) comment on and provide the natural (stable) concentrations of Sr, Ni, Co, and Cs being studied in the original groundwater, (3) provide the mineralogy of the site sediments especially for the silt and clay fractions, (4) comment on whether the procedure required the pH of the blank spike test tubes to also be neutralized with sodium hydroxide back to pH values closer to the native sediment / distilled water 1:1 slurry pH values, (5) comment on the energy levels for which each radionuclide was quantified, (6) comment on and provide the measured or estimated macro chemical composition and pH of waste liquid(s).

(B) (7) footnote column "10% probability K_d" entries in Table 2.4S13.4 to identify their origin (the values do not appear in NUREG/CR 6697), (8) further justify the use of non-site-specific K_d data and the 10th percentile value in particular as opposed to a lower value, and (9) correct the truncated half-life of Pu239 in Figure 2.4S.13-1.

Response:

The requested information regarding the K_d report previously provided in response to RAI 02.04.13-7 is provided below. This clarification is provided as numbered items that correspond with the nine numbered items in the NRC RAI.

(A)(1) The secondary stock solutions were created from a set of instructions entitled "Making Spike Solution for STP K_d Project," dated September 10, 2007 (file "Spike Solution for STP v2.doc"), which is provided at the top of the following page of this response. As indicated in these instructions, three secondary stock solutions were prepared from primary stock solutions (purchased from Eckert & Ziegler Analytics in Atlanta, Georgia). The secondary stock solutions were:

- Fe-55 and Pu-238
- Ni-59
- Co-57, Cs-137 and Sr-85

These solutions were then of the proper dilution for use in the K_d test, that is, 170 μL aliquots could be added from any stock solution and have the appropriate starting concentrations. The following instructions include details of how the dilutions were prepared.

“Spike Solution for STP v2.doc.”

Making Spike Solution for the STP Kd Project

Dan Kaplan, 9/10/2007

Three spike solutions will be made:

- Fe-55 & Pu-238,
- Ni-59,
- Co-57, Cs-137, Sr-85,

Fe-55 and Pu-238 Spike Solution.

1. For the first spike solution, add the following spike volumes to make a spike mixture. Mix solution well.

Element	Isotope	Stock Sol'n			Vol. to add to spike mixture (mL)
		Remaining Vol. (mL)	Activity (μCi)	Conc. ($\mu\text{Ci/mL}$)	
Fe	55	4.5	5	1	4.5
Pu (Hobbs)	238	5	10	2	2.5
1 M HNO₃					0.6
Total					7.6

2. Add 170 μL of this mixture to each tube (start with blanks). Do not add any spike to the blank controls (122c-A & 122c-B).

Ni-59 Spike Solution

3. Be sure you use the correct isotope, we have two Ni isotopes in our hood. For the first spike solution, add the following spike volumes to make a spike mixture. Mix well.

Element	Isotope	Stock Sol'n			Vol. to add to spike mixture (mL)
		Remaining Vol. (mL)	Activity (μCi)	Conc. ($\mu\text{Ci/mL}$)	
Ni	59	5	0.1	0.01	5.0
1 M HNO₃					2.6
Total					7.6

1. Add 170 μL of this mixture to each tube (start with blanks). Do not add any spike to the blank controls (122b-A & 122b-B).

Co-57, Cs-137, and Sr-85 Spike Solution

1. Add spike stock solutions to 1N HNO₃. Be sure you use the correct isotope. Mix solution well.

Element	Isotope	Stock Sol'n			Vol. to add to spike mixture (mL)
		Remaining Vol. (mL)	Activity (μCi)	Conc. (μCi/mL)	
Co	57	4.9	50	10	0.1
Cs	137	4.9	50	10	0.1
Sr	85	9.8	50	5	0.2
1 N HNO₃					6.2
Total					7.6

2. Add 170 μL of this mixture to another set of tube (start with blanks). Do not add any spike to the blank controls (122a-A & 122a-B).

- (A)(2) The groundwater was not analyzed for natural (stable) concentrations of Sr, Ni, Co, and Cs. However, these isotopes were most likely present at quantities greater than those used to measure the K_d values. Their presence likely lowered the K_d value compared to similar tests conducted without their presence, for example, those conducted in distilled de-ionized water. The reason for this is because these stable isotopes compete for the same sorption sites as the radioisotope being introduced for the K_d test. Consequently, omitting the quantification of stable isotopes does not lead to overestimating K_d values.
- (A)(3) The clay mineralogy (such as measured by XRD) of the specific sediment samples used in the K_d measurements was not measured. As documented in Table 2.4S.13-3, “Laboratory Distribution Coefficient Measurements in mL/g for the Lower Shallow Aquifer,” of the STP Units 3 and 4 FSAR (COLA, Part 2 [Tier 2]), the sediment samples used in the K_d measurements were from the Lower Shallow Aquifer.

As illustrated in FSAR Figure 2.4S.12-29; “Simplified Hydrostratigraphic Section,” the geologic materials of the Lower Shallow Aquifer are silty sand and poorly graded sand with thin clay and silt layers. FSAR Section 2.4S.12.1.3, “Local Hydrogeology,” describes the Beaumont Formation within the Chicot Aquifer as the principal water-bearing unit used for groundwater supply in the vicinity of the STP site. The Beaumont Formation is further described in FSAR Section 2.4S.12.1.2.1, “Beaumont Formation.” The Beaumont is a heterogeneous formation, containing thick interbedded layers of clay, fine sand, and silt. The clay fraction is primarily composed of montmorillonite, illite, kaolinite, and fine-grained quartz. The process of desiccation has consolidated the clay present in the formation. The sands and silts, which vary in compactness from loose to very dense, are composed of quartz, feldspars, and large particles of kaolinite, calcite, and occasionally hornblende [References (A)(3)-1 and (A)(3)-2].

References:

- (A)(3)-1 Environmental Assessment Report, Port of Texas City/Texas City Terminal Railway Hazardous Material Railcar Storage, Port of Texas City, Texas. Prepared for Don Fairley, Regional Environmental Officer FEMA Region VI Denton, TX. Prepared by InControl Technologies, Inc., Houston, Texas, December 18, 2007.
- (A)(3)-2 Bureau of Economic Geology, Geologic Map of Texas: University of Texas at Austin, 1992.
- (A)(4) The procedure required that the pH of the blank spike test tube be neutralized to that of a sediment: groundwater suspension. The reason for this requirement is to have the “control blank” treated identically to that of the sediment samples.

(A)(5) The energy levels for each radionuclide were quantified as follows:

<u>Radionuclide</u>	<u>Energy</u>	<u>Radionuclide</u>	<u>Energy</u>
Co-57	122.1 keV	Fe-55	5.9 keV
Cs-137	661.6 keV	Ni-59	6.9 keV
Sr-85	514.0 keV	Pu-238	13.6 keV

(A)(6) Groundwater will be used as the starting solution for STP processes. The table below provides the macro chemical composition of groundwater reported for a relatively recent (12/31/2006) sample taken from the STP site. There is nothing especially outstanding about this groundwater. It is a near neutral pH groundwater that is dominated by carbonate and chloride anions and sodium and calcium cations. The calculated charge balance of the solution is near perfect, i.e., charge imbalance is only 1.8 percent, providing one indication that the major constituents are accounted for in the analyses. The ionic strength of the solution – 0.022 molar – is not unexpected for such geologic systems.

Example of the Groundwater Chemistry at the STP Upper Aquifer (Well OW-934U, 12/31/2006 found in FSAR Table 2.4S.12-16)	
pH	6.91
Specific Conductance ($\mu\text{mhos/cm}$)	1891
Total Alkalinity (mg/L as CaCO_3)	378
Ca (mg/L)	87.8
Mg (mg/L)	56.2
Na (mg/L)	218
Cl^- (mg/L)	412
SO_4^{2-} (mg/L)	47.3
F^- (mg/L)	1.4
NO_3^- (mg/L)	0.163
K (mg/L)	Below Detection Limit
Charge imbalance (%) ^(a)	1.8
Ionic Strength (mol/L) ^(a)	0.022

^(a) Calculated using MINTEQA2 (Win V1.5). Details are provided at the end of this response to RAI Item (A)(6).

An estimated composition of the waste liquid would likely be a more dilute version of the chemistry presented in the table above because the groundwater in the Low Conductivity Waste (LCW) collector tank will be put in contact with something that will decrease the ionic strength, such as a mixed bed of cation and anion resins, or a deionizer membrane.

The K_d values were measured using STP groundwater and sediment. The intent of using STP groundwater was to simulate radionuclides geochemical conditions in the far field. The near field conditions for the rupture of the LCW collector tank would be best simulated by using the same sediment but with an aqueous phase with less salts. The

question then is, what is the general effect of lowering the ionic strength on K_d values? Often, at higher ionic strengths there is less sorption because of greater competition for sorption by the other cations and anions in solution. (There are exceptions that would not apply to groundwater conditions. When ‘indifferent ions’ are present, i.e., ions that do not interact with surfaces and simply influence aqueous charge properties, such as perchlorate, it is possible that this statement does not apply. The increase in ionic strength collapses the double layer promoting greater contact with the sorbing cation [radionuclide] and the sediment surface.) An example of this is presented in Dzombak and Morel [Reference (A)(6)-1]. Consequently, in the LCW near field, it seems reasonable to anticipate that K_d values would be either the same or temporarily somewhat greater than those measured for the far field conditions.

Reference:

- (A)(6)-1 Dzombak, D. A. and Morel, F. M. M. Surface Complexation Modeling: Hydrous Ferric Oxide, John Wiley-& Sons, Inc, New York, pp. 260 and 276, 1990.

MINTEQA2 Thermodynamic Speciation Modeling Calculations of STP Groundwater

STP Groundwater (OW-934U_12/31/2006)

SUMMARY OUTPUT -- Date and Time: 9/3/2009 10:59:37 AM

STP Groundwater (OW-934U_12/31/2006)

System pH: 6.91
Ionic Strength: 2.244E-02 mol/L
 Temperature: 25.0 Deg C
Charge Imbalance: 1.8 Percent

Species in Solution	Molar Concentration
H+1	1.423E-07
Ca+2	2.074E-03
Mg+2	2.187E-03
Na+1	9.463E-03
CO3-2	2.923E-06
SO4-2	3.792E-04
NO3-1	2.622E-06
Cl-1	1.166E-02
F-1	6.391E-05
NaCO3-	2.880E-07
NaHCO3 (aq)	1.964E-05
OH-	9.460E-08
MgOH+	1.887E-08
CaOH+	2.189E-09
HF (aq)	1.000E-08
HF2-	2.443E-12
H2F2 (aq)	2.695E-16
MgF+	8.768E-06
CaF+	8.089E-07
NaF (aq)	2.839E-07
HSO4-	2.927E-09
MgSO4 (aq)	4.693E-05
CaSO4 (aq)	5.604E-05
NaSO4-	1.078E-05
CaNO3+	9.617E-09
HCO3-	4.968E-03
H2CO3 (aq)	1.181E-03
MgCO3 (aq)	1.897E-06
MgHCO3+	7.064E-05
CaHCO3+	5.969E-05
CaCO3 (aq)	2.679E-06

Component Distribution Among Species:

For Component: F-1

86.6% is in species: F-1
 11.9% is in species: MgF+
 1.1% is in species: CaF+

For Component: Ca+2

94.6% is in species: Ca+2
 2.6% is in species: CaSO4 (aq)
 2.7% is in species: CaHCO3+

For Component: Mg+2

94.5% is in species: Mg+2
 2.0% is in species: MgSO4 (aq)
 3.1% is in species: MgHCO3+

For Component: Na+1

99.7% is in species: Na+1

For Component: CO3-2

78.8% is in species: HCO3-
 18.7% is in species: H2CO3 (aq)
 1.1% is in species: MgHCO3+

For Component: SO4-2

76.9% is in species: SO4-2
 9.5% is in species: MgSO4 (aq)
 11.4% is in species: CaSO4 (aq)
 2.2% is in species: NaSO4-

For Component: NO3-1

99.6% is in species: NO3-1

For Component: Cl-1
 100.0% is in species: Cl-1

Component Distribution Among Phases

----- Percent in Each Phase -----

	Dissolved	Sorbed	Precipitated
For Component: F-1	100.0%	0.0%	0.0%
For Component: Ca+2	100.0%	0.0%	0.0%
For Component: Mg+2	100.0%	0.0%	0.0%
For Component: Na+1	100.0%	0.0%	0.0%
For Component: CO3-2	100.0%	0.0%	0.0%
For Component: SO4-2	100.0%	0.0%	0.0%
For Component: NO3-1	100.0%	0.0%	0.0%
For Component: Cl-1	100.0%	0.0%	0.0%
For Component: H+1	100.0%	0.0%	0.0%

(B)(7) The contents of Table 2.4S.13-4 are changing from Revision 2 to Revision 3 of the STP COLA, and the column in Table 2.4S.13-4 for which the RAI requests a footnote will not appear in Revision 3. The following explains the derivation of the values in the column titled “10% probability K_d ”:

The 10th percentiles of the K_d probability distributions for each radionuclide of concern were determined from the lognormal K_d probability distributions listed in Reference (B)(7)-1 using the LOGINV function, which calculates the inverse of the lognormal cumulative probability distribution for any specified percentile of the distribution, given its mean and standard deviation. No K_d probability distribution for Y is available from Reference (B)(7)-1. The value shown is the 10th percentile of the lognormal K_d probability distribution for scandium (adjacent to yttrium in the periodic chart) provided in Reference (B)(7)-1.

Reference:

(B)(7)-1 “Development of Probabilistic RESRAD 6.0 and RESRAD-BUILD 3.0 Computer Codes”, NUREG/CR-6697, Attachment C, Table 3.9-1, Yu, C., LePoire, D., Gnanapragasam, E., Arnish, J., Kamboj, S., Biwer, B.M., Cheng, J-J, Zilen, A., and Chen, S.Y., Argonne National Laboratory, 2000.

(B)(8) A preliminary screening radionuclide transport analysis was conducted to determine which radionuclides required laboratory analyses of soil samples to determine site-specific K_d values. The screening transport analysis evaluated which radionuclides would be present at concentrations greater than their respective effluent concentration limits (ECLs) at the point of compliance after a postulated spill, assuming radioactive decay was the only attenuating mechanism. That analysis used preliminary estimated values of hydraulic gradient, effective porosity and hydraulic conductivity to estimate groundwater velocity and travel time to the point of compliance. The analysis resulted in the conclusion that Fe-55, Co-60, Ni-63, Sr-90, Cs-137, and Pu-239 would require determination of site-specific K_d values.

After results of the subsurface investigation became available and values for the hydraulic gradients, effective porosity, and hydraulic conductivity more representative of measured site conditions were determined, a more conservative transport analysis was completed, comparing radionuclide concentrations at the point of compliance to 1 percent of their ECLs. The results of this more conservative analysis determined that Y and Np were also radionuclides of concern. However, the laboratory analysis to determine site-specific K_d values had been completed by this time, so K_d values for Y and Np were derived from the literature. No probability distributions from which K_d values for Y can be determined are available from Reference (B)(8)-1, so the probability distribution from Reference (B)(8)-1 for the element adjacent to Y in the periodic chart (Sc) was used, with the assumption that the properties of the two elements are similar.

For those radionuclides for which K_d values were determined by laboratory analysis, the geometric mean of the results of 10 sample analyses was used in the transport analysis to best represent the soils in the Upper and Lower Shallow Aquifers. K_d probability distributions in Reference (B)(8)-1 are derived from various studies cited in the literature. These studies evaluated a wide range of soil types. However, the soils in the Upper and Lower Shallow Aquifers at STP are primarily sandy, which generally yield distribution coefficients lower than those measured in other soil types such as silt, clay and loam.

Therefore, to provide a conservative analysis, the 10th percentiles of the K_d probability distributions for Sc and Np from Reference (B)(8)-1 were used in the transport analysis rather than the geometric means of their distributions. The objective of the analysis was to use the most representative K_d values rather than the minimum values, and engineering judgment was relied upon to choose the 10th percentile of the K_d probability distributions in Reference (B)(8)-1 as representative of sandy soil. Table 2.4S.13-4 of the STP COLA, Revision 2, shows that the 10th percentile values of the K_d probability distributions from Reference (B)(8)-1 are generally lower than the geometric means of the site-specific K_d values for the corresponding radionuclides. This confirms that use of the 10th percentile K_d values provides a conservative and plausible analysis.

Reference:

(B)(8)-1 “Development of Probabilistic RESRAD 6.0 and RESRAD-BUILD 3.0 Computer Codes”, NUREG/CR-6697, Attachment C, Table 3.9-1, Yu, C., LePoire, D., Gnanapragasam, E., Arnish, J., Kamboj, S., Biwer, B.M., Cheng, J-J, Zilen, A., and Chen, S.Y., Argonne National Laboratory, 2000.

(B)(9) Figure 2.4S.13-1 of the STP Units 3 and 4 FSAR will be revised to show the half-life of Pu-239 as 2.4 E+004 years, as indicated in the markups provided at the end of this RAI response.

As discussed in Item (B)(9) above, FSAR Figure 2.4S.13-1 will be revised as indicated by the “cloud” marking in the figure markup provided on the following page.

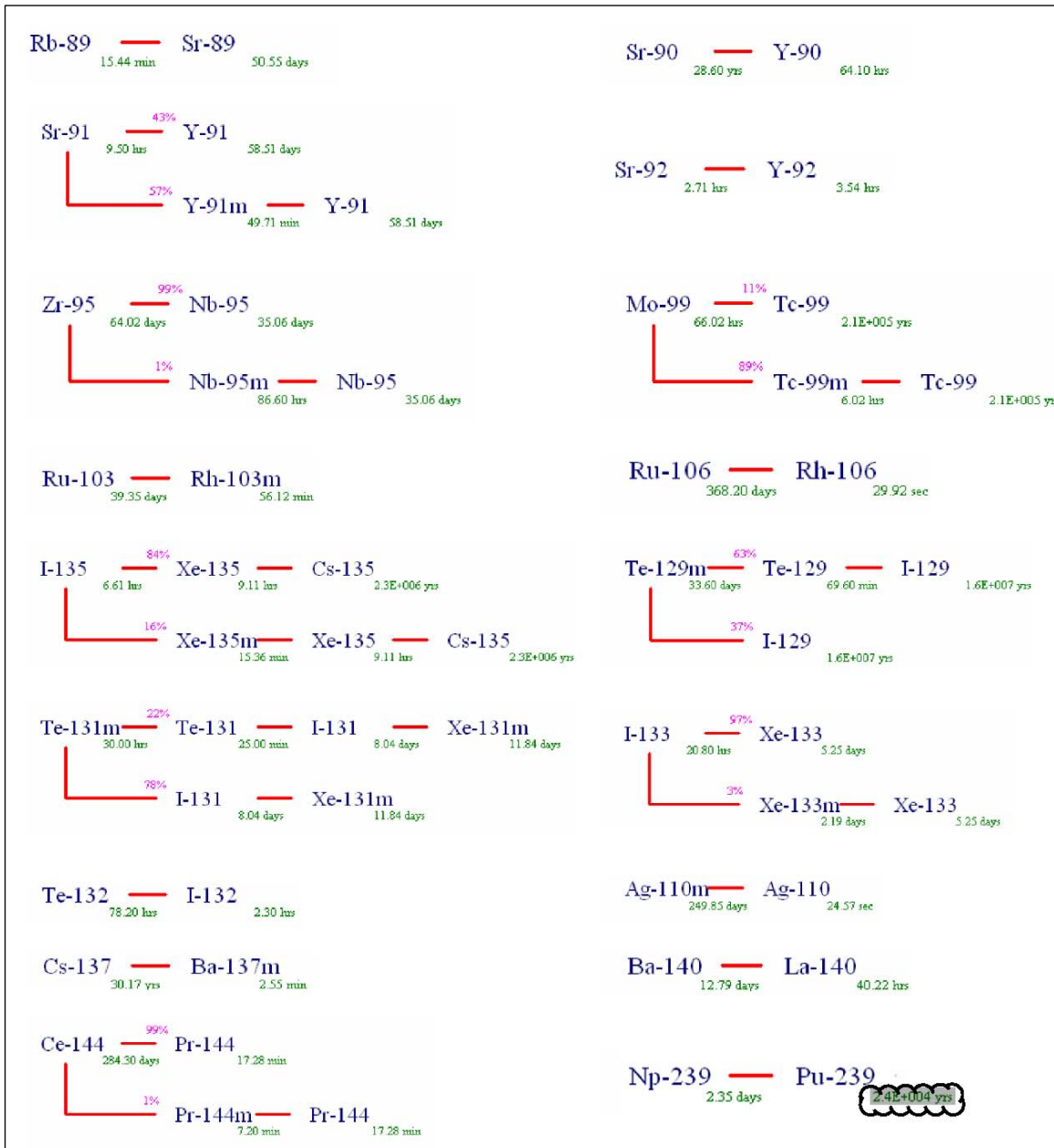


Figure 2.4S.13-1 Decay Chains Considered in Accidental Effluent Release

RAI 02.04.13-13**Question:**

(A) In its review of the applicant's response to RAI 02.04.13-9, the staff noted that the applicant, STP, (1) does not clearly state the future text revisions, (2) nor does the applicant provide a quantitative statement regarding potential impact. Regarding item (1); in Rev 2 of the application, reference to the Radwaste Building being a Seismic Category I building has been stricken; however, in the RAI response it appears being a Seismic Category I building is significant and the descriptor is retained. Regarding item (2); some technical assumptions and quantification regarding the release and its dilution are needed to support the conclusion in Section 2.4S.13.2 that "A flood of this magnitude would disperse and dilute the radionuclide concentration of a surface water spill."

(B) In addition, it is not clear that the applicant has considered the water quality of the MCR water itself in the qualitative statement cited above because the UFSAR for STP Units 1&2 states the expected maximum reservoir tritium concentration is 21,000 pCi/L. Staff request that the applicant clarify item (1), and provide a quantitative analysis supporting item (2). The staff notes that because dilution is involved in the scenario, a minimum flood volume would provide higher concentrations, and impacts at the boundary of the site are of greater interest than a far-field point of exposure. During the safety site audit, the applicant described the use of modular treatment facilities within the open bay of the Radwaste Building, and the role they could play in a release during an MCR dike breach flood. Since they are not mentioned in the response to RAI 02.04.13-09, the staff requests a description of the process used to eliminate facilities potentially containing liquid waste in the building bay from the analysis.

Response:

(A)(1) The response to RAI 02.04.13-9 retained the original text that indicated that the Radwaste Building is Seismic Category I. This is no longer the case. Instead, the Radwaste Building is designed to meet the requirements of Regulatory Guide 1.143. The text for COLA FSAR section 2.4.13.2 provided in the response to RAI 02.04.13-9 and included in COLA FSAR Revision 3 will be revised to remove the Seismic Category I descriptor and replace it with a reference to Regulatory Guide 1.143.

(A)(2) The Radwaste Building is designed so that essentially all of the radioactive liquid is stored in tanks that are below grade. The dispersal of a significant amount of liquid radioactive waste following an MCR dike breach flood therefore requires two failures, the failure of the dike and the failure of a radwaste tank. Both of these failures have a very low probability, and the simultaneous occurrence of both failures would not be considered a normal design basis event. However, to respond to this question, an approximate quantitative evaluation of this event is provided. This evaluation is limited to the MCR dike breach flood. The potential for flooding the Radwaste Building following other flood events is addressed in the response to RAI 02.04.13-14.

The MCR dike breach flood scenario results in a flood elevation that could be as high as El. 38.8'. Since the floor of the Radwaste Building is at El. 35', the flood water would be

above the Radwaste Building floor. Therefore, it is assumed that the entire Radwaste Building, including the basement, is flooded up to an elevation of 38.8 ft. Then it is assumed that a radwaste tank fails and the contents of the tank are mixed in the floodwater. This results in contaminated floodwater above the ground floor of the Radwaste Building. As the flood water recedes, the contaminated water in the Radwaste Building above the ground floor flows out of the building and is diluted by the floodwater on the site before reaching the site boundary.

The objective of the approximate evaluation is to estimate the activity concentrations in the floodwater at the site boundary to determine if the concentrations would exceed the effluent concentration limits (ECL) in 10 CFR 20. The activity released is the design basis activity in the Low Conductivity Waste (LCW) Collector Tank, which contains the largest liquid inventory of radioactivity in the Radwaste Building. This activity is diluted by two mechanisms. First, the floodwater that enters the Radwaste Building will dilute the activity released from the tank. Although there is no flow mechanism that would cause the activity in the basement of the Radwaste Building to move upwards out of the basement, it is conservatively assumed that the activity is distributed in all of the floodwater, including the floodwater above the ground floor in the Radwaste Building. Since the volume of the LWC Collector Tank is 4940 cubic feet (140 m^3), and the approximate floodwater volume in the Radwaste Building is 883,000 cubic feet (25000 m^3), the dilution factor is approximately 178.

A second dilution factor occurs as the contaminated liquid flows out of the Radwaste Building and mixes with the floodwater outside the Radwaste Building. The MCR has a surface area of 7000 acres with storage volume of 202,700 acre feet at the operating level of 49 ft. The MCR dike breach analysis at STP Units 3 & 4 was performed and presented in Reference 1. In this analysis a postulated failure of the MCR dike with trapezoidal breach having bottom width of 380 ft at elevation 29 ft and side slope of 1H:1V was analyzed. An initial MCR water level of 50.9 ft was assumed at the time of breach. Two breach scenarios, east breach and west breach were considered to determine the effect of the breach on Unit 3 and Unit 4 respectively. Based on the analysis presented in Reference 1, MCR breach would result in a flood with peak discharge of 130,000 cubic feet per second downstream of the breach. Floodwater from the MCR breach will flow through the area encompassing proposed Units 3 & 4 and Units 1 & 2 and will spread into the area bounded by FM 521 road to the north of the site. The area surrounding the STP Units 3 & 4 has an approximate existing grade elevation varying from 25 ft to 30 ft. The proposed grade elevation at the Radwaste Building is 34 ft. and the building floor is at El. 35'. North of FM 521 and west of the West MCR embankment there are levees. The flood water from the MCR breach will flow north towards the units and part of the water will flow towards east to the Colorado River. The other part of the flood water will flow to the west and will reach the Little Robins Slough. This flood water will flow through the Little Robins Slough along the west embankment of the MCR and flow east ward south of the MCR and ultimately flows to the intracoastal water way near the Gulf of Mexico.

The flood hydrograph through the MCR breach after initiation of the breach is presented in Table 2.4S.4-6 of Reference 1. As shown in the table, breach flow rapidly increases to 130,000 cubic feet per second in 1.7 hours and gradually reduces to 14,840 cubic feet per second at 30 hours from start of the breach. Similarly the MCR water level drops from initial water level of 50.9 ft. to 34 ft at 30 hours from start of the breach. It is assumed that at the end of 30 hours the water level at the Radwaste Building will be approximately 34 ft or slightly lower. Water levels at different plant facilities associated with the East and West breaches are presented in Reference 1. The maximum water level near the plant buildings due to the MCR dike breach is 38.8 ft, which is used in the present analysis.

Contaminated water will flow out of the Radwaste Building once the water level surrounding the building starts to drop. The total volume of contaminated water will be the volume in the building between elevations 38.8 ft and 35 ft, which is 97,000 cubic feet. This volume of contaminated water will mix with a portion of the flood water volume outside the Radwaste Building and will flow away from the building. To provide quantitative estimate of dilution it is assumed that the flood volume flowing out of the breach will split into two halves. One half flows east towards Colorado River and does not interact with the Radwaste Building and is not contaminated with leakage from the Radwaste Building. The second half flows west towards Little Robins Slough, and for this analysis only the dilution due to the second half of the flood volume is investigated. The total volume of water out of the breach from the start of the breach until 30 hours after the breach is estimated as 118,260 acre feet. The half of this volume that flows towards the west will be 59,130 acre feet. Conservatively assuming only 4% of this volume mixes with the 97,000 cubic feet of contaminated water from the Radwaste Building will yield a dilution factor greater than 1000. Note that even after the 30-hour period there will be flow out of the MCR from El. 34' to the bottom of the breach elevation of 29 ft, which will provide additional dilution.

The attached table is a list of the activity in the LCW Collector Tank. The activity is converted to a concentration outside the Radwaste Building by dividing by the tank volume and the dilution factors identified above. Per SRP 15.7.3, the criteria in Part 20 were conservatively used as the acceptance criteria, even though the postulated event is not credible (i.e., MCR failure with a concurrent failure of the tank). The fraction of the 10 CFR 20 ECL is computed and summed. Since the sum of the fractions is less than one, this table demonstrates that the concentrations resulting from this approximate evaluation of the effect of the MCR dike breach and the resulting flooding of the Radwaste Building are a small fraction of the 10 CFR 20 limits.

- (B) A clarification of the description of the seismic classification of the Radwaste Building is provided in the FSAR markup below.

An approximate quantitative evaluation of the dilution of a release from the Radwaste Building following an MCR dike breach flood is summarized above and in the attached table. Note that these results are for dilution on site in the immediate vicinity of the Radwaste Building and do not take into consideration any additional dilution that may

occur off site, such as in the intracoastal water-way. The last two columns of the attached table contain the activity concentrations in the MCR as listed in Table 11.A-1 of the STP 1 & 2 UFSAR. The increase in activity in the MCR due to the operation of STP 3 & 4 will not be significant because most of the liquid waste is recycled and the amount of tritium produced by the ABWR is much less than the tritium produced by STP 1 & 2. The fraction of the 10 CFR 20 ECL in the MCR water is less than the fraction in the contaminated water released from the Radwaste Building following the MCR dike breach flood and tank failure scenario, and the combined fraction of the 10 CFR 20 ECL is significantly less than 1. Therefore, the quality of the water in the MCR does not affect the conclusion of the approximate quantitative evaluation presented above.

The current design of the Radwaste Building includes processing equipment on the ground floor of the Radwaste Building. The flooding could cause electrical damage to this equipment, but would not cause a breach the system due to protection afforded by the building and internal shield walls. Additionally, since the equipment would not be operating following the MCR dike breach, there would be no motive force to move contaminated liquid from the tanks located in the basement to the area above the floor even if an equipment breach occurred. Therefore, the failure of the tank described above is the limiting failure for the MCR dike breach flood.

Reference 1. RAI response to question 02.04.04-9 and attached proposed COLA revisions (U7-C-STP-NRC-090012, February 23, 2009; Attachment 1)

The update to the first paragraph of FSAR Section 2.4S.13.2, identified in RAI 02.04.13-9, and included in Revision 3 of the COLA FSAR will be revised as follows:

The design of the Liquid Radioactive Waste System (LWMS) for STP 3 & 4 as described in Section 11.2 specifies that all liquid radwaste tanks are to be contained inside of the Radwaste Building. The Radwaste Building, which is designed in accordance with Regulatory Guide 1.143, will have Seismic Category 4 walls and basemat of sufficient dimensions to contain all liquid radwaste. There are no outdoor tanks in the LWMS that could release radioactive effluent. Therefore, the most plausible a postulated accident scenario involving that could result in the release of effluent directly to surface water is a rapid and catastrophic flood, such as that caused by a breach of the MCR embankment, inundating the Radwaste Building coinciding with leakage from the indoor tanks on the basement level of the Radwaste Building.

Activity Released From the Radwaste Building Following an MCR Dike Breach						
Isotope	MBq	Release Concentration $\mu\text{Ci/cc}$	ECL $\mu\text{Ci/cc}$	ECL Ratio	MCR Concentration $\mu\text{Ci/cc}$	ECL Ratio
Halogens						
I-131	2.03E+04	2.19E-08	1.00E-06	2.19E-02	2.20E-10	2.20E-04
I-132	8.06E+03	8.70E-09	1.00E-04	8.70E-05		
I-133	5.54E+04	5.98E-08	7.00E-06	8.55E-03	1.20E-16	1.71E-11
I-134	5.28E+03	5.70E-09	4.00E-04	1.43E-05		
I-135	2.50E+04	2.70E-08	3.00E-05	9.00E-04	3.90E-31	1.30E-26
Soluble Fission Products						
Rb-89	9.42E+01	1.02E-10	9.00E-04	1.13E-07		
Sr-89	2.11E+03	2.28E-09	8.00E-06	2.85E-04	6.30E-13	7.88E-08
Sr-90	2.67E+02	2.88E-10	8.00E-07	3.60E-04	6.40E-13	8.00E-07
Y-90	2.67E+02	2.88E-10	7.00E-06	4.12E-05		
Sr-91	3.33E+03	3.60E-09	2.00E-05	1.80E-04	8.90E-28	4.45E-23
Sr-92	2.57E+03	2.78E-09	4.00E-05	6.94E-05		
Mo-99	8.86E+03	9.57E-09	2.00E-05	4.78E-04	2.50E-13	1.25E-08
Tc-99m	8.86E+03	9.57E-09	1.00E-03	9.57E-06	5.70E-34	5.70E-31
Te-129m	7.13E+02	7.70E-10	7.00E-06	1.10E-04	1.90E-12	2.71E-07
Te-131m	2.25E+02	2.43E-10	8.00E-06	3.04E-05	1.80E-17	2.25E-12
Te-132	5.09E+02	5.50E-10	9.00E-06	6.11E-05	2.00E-13	2.22E-08
Cs-134	4.00E+02	4.32E-10	9.00E-07	4.80E-04	4.60E-09	5.11E-03
Cs-136	1.35E+02	1.46E-10	6.00E-06	2.43E-05	8.80E-12	1.47E-06
Cs-137	1.22E+03	1.32E-09	1.00E-06	1.32E-03	1.00E-08	1.00E-02
Cs-138	5.46E+02	5.90E-10	4.00E-04	1.47E-06		
Ba-140	5.04E+03	5.44E-09	8.00E-06	6.80E-04	9.80E-14	1.23E-08
Np-239	3.20E+04	3.46E-08	2.00E-05	1.73E-03	3.30E-16	1.65E-11
Insoluble Fission Products						
Y-91	2.97E+04	3.21E-08	8.00E-06	4.01E-03	1.10E-13	1.38E-08
Y-92	2.32E+03	2.51E-09	4.00E-05	6.26E-05		
Y-93	2.72E+04	2.94E-08	2.00E-05	1.47E-03	1.70E-28	8.50E-24
Zr-95	6.03E+03	6.51E-09	2.00E-05	3.26E-04	3.50E-12	1.75E-07
Nb-95	6.03E+03	6.51E-09	3.00E-05	2.17E-04	2.60E-12	8.67E-08
Ru-103	1.38E+04	1.49E-08	3.00E-05	4.97E-04	2.50E-13	8.33E-09
Rh-103m	1.38E+04	1.49E-08	6.00E-03	2.48E-06		
Ru-106	2.69E+03	2.91E-09	3.00E-06	9.68E-04	3.10E-11	1.03E-05
Rh-106	2.69E+03	2.91E-09	1.00E-04	2.91E-05		
La-140	1.89E+05	2.04E-07	9.00E-06	2.27E-02	5.10E-17	5.67E-12
Ce-141	2.04E+04	2.20E-08	3.00E-05	7.34E-04	6.10E-14	2.03E-09
Ce-144	2.66E+03	2.87E-09	3.00E-06	9.58E-04	5.10E-11	1.70E-05
Pr-143	2.66E+03	2.87E-09	2.00E-05	1.44E-04	1.60E-14	8.00E-10

Activity Released From the Radwaste Building Following an MCR Dike Breach						
Isotope	MBq	Release Concentration $\mu\text{Ci/cc}$	ECL $\mu\text{Ci/cc}$	ECL Ratio	MCR Concentration $\mu\text{Ci/cc}$	ECL Ratio
Activation Products						
Na-24	1.29E+04	1.39E-08	5.00E-05	2.79E-04		
P-32	2.65E+03	2.86E-09	9.00E-06	3.18E-04		
Cr-51	1.04E+05	1.12E-07	5.00E-04	2.25E-04	1.10E-10	2.20E-07
Mn-54	2.21E+03	2.39E-09	3.00E-05	7.96E-05	1.20E-10	4.00E-06
Mn-56	1.17E+04	1.26E-08	7.00E-05	1.81E-04		
Co-58	4.43E+03	4.78E-09	2.00E-05	2.39E-04	8.00E-10	4.00E-05
Co-60	1.47E+04	1.59E-08	3.00E-06	5.29E-03	1.80E-09	6.00E-04
Fe-55	1.09E+04	1.18E-08	3.00E-04	3.92E-05	7.70E-12	2.57E-08
Fe-59	6.02E+02	6.50E-10	1.00E-05	6.50E-05	2.00E-11	2.00E-06
Ni-63	3.79E+04	4.09E-08	1.00E-04	4.09E-04		
Cu-64	3.17E+04	3.42E-08	2.00E-04	1.71E-04		
Zn-65	6.00E+03	6.48E-09	5.00E-06	1.30E-03		
Ag-110m	3.01E+01	3.25E-11	6.00E-06	5.42E-06		
W-187	5.66E+02	6.11E-10	3.00E-05	2.04E-05		
H3			1.00E-03		2.10E-05	2.10E-02
			Total	7.80E-02		3.70E-02

RAI 02.04.13-14**Question:**

In the review of the applicant's response to RAI 02.04.13-10, the staff noted that the applicant proposed changes to the FSAR text including the sentence, "The local PMP storm potentially could result in release of the greatest concentration of radioactive material to the environment because the flood level from this event would be lower than that from the three other flood mechanisms, and, therefore, would provide less dilution if the material were to escape the Radwaste Building." Staff has reviewed the information presented and determined that the local PMP storm with an estimate maximum water level of 36.6 ft MSL is the highest of the four events evaluated, not the lowest. The staff request that the applicant review and revise the aspect of the RAI response and proposed changes to the FSAR.

Response:

This RAI response reflects results from the revised MCR embankment breach analysis and the revised wave run-up analysis on the flood level for the Colorado River cascading dam failures described in the response to RAI question 02.04.04-9 and attached proposed COLA revisions (U7-C-STP-NRC-090012, February 23,2009; Attachment 1).

The design basis flooding (DBF) elevation for the STP 3 & 4 site is determined by considering a number of different flooding scenarios. The flooding scenarios potentially applicable and investigated for the site include the following: local probable maximum precipitation (PMP) at the site, cascading dam failure on the Colorado River, MCR embankment breach, probable maximum flood (PMF) on streams and rivers, probable maximum surge and seiche (PMSS), probable maximum tsunami (PMT), flooding due to ice effects, and flooding caused by channel diversions. In applicable cases the flooding scenarios were investigated in conjunction with other flooding and meteorological events, such as wind- generated waves and tidal levels, as recommended in the guidelines presented in ANSI/ANS 2.8-1992 (COLA FSAR Reference 2.4S.2-9). Detailed discussions on each of these flooding events and how they were estimated are found in Subsections 2.4S.2 through 2.4S.7, and Subsection 2.4S.9. The estimated flood elevations are based on the site plan provided in the COL application.

The following is a summary of the maximum flood levels resulting from external flood events affecting the STP 3 & 4 Site, excluding the MCR embankment breach. Ice effect and channel diversions do not pose a flooding risk to the STP 3 & 4 Site, as described in COLA Subsections 2.4S.7 and 2.4S.9, respectively.

1. Local PMP Event (COLA Subsection 2.4S.2):
 - maximum water surface elevation = 36.6 ft MSL
 - this maximum flood level is 1.6 ft above the plant building floor elevation of 35.0 ft
2. Cascading Dam Failure on the Colorado River (COLA Subsection 2.4S.4):
 - maximum water surface elevation = 28.6 ft MSL
 - maximum flood level including wind-wave action = 34.4 ft MSL
 - this maximum flood level is below the plant building floor elevation of 35.0 ft

3. PMF Water Level on the Colorado River (COLA Subsection 2.4S.3):
 - maximum water surface elevation = 26.3 ft MSL
 - maximum flood level including wind-wave action = less than 34.4 ft MSL (dam failure flood elevation)
 - this maximum flood level is below the plant building floor elevation of 35.0 ft
4. PMH in the Gulf of Mexico (COLA Subsection 2.4S.5):
 - maximum water surface elevation = 31.1 ft MSL
 - maximum flood level including wind-wave action = less than 34.4 ft MSL (dam failure flood elevation)
 - this maximum flood level is below the plant building floor elevation of 35.0 ft
5. PMT at STP 3 & 4 Site (COLA Subsection 2.4S.6):
 - maximum water surface elevation = 16.3 ft MSL
 - maximum flood level including wind-wave action = less than 34.4 ft MSL (dam failure flood elevation)
 - this maximum flood level is below the plant building floor elevation of 35.0 ft

As discussed above, of the several flooding mechanisms considered above, the local PMP storm is the only mechanism having the potential to flood the Unit 3 and Unit 4 Radwaste Buildings, where the postulated accident described in Section 2.4S.13.1.1 occurs. The maximum water level in the power block area due to a local PMP storm event is estimated to be at elevation 36.6 ft MSL, which is higher than the ground floor elevation of 35 ft MSL at the Radwaste Buildings. Thus, the PMP event could potentially flood the Radwaste Building. The local PMP storm event can be considered a slow-moving event for which advance notice would be available. For this reason, there would be opportunity to initiate operator action to mitigate potential flooding effects. Therefore, it is unlikely that the PMP event would flood the Radwaste Building.

Based on the above discussion, none of the flooding mechanisms considered presents a credible risk of environmental contamination.

The following shows portions of COLA FSAR Section 2.4S.13.2, Revision 3, which is scheduled to be submitted in September 2009. Proposed changes to Revision 3 of COLA FSAR Section 2.4S.13.2 are highlighted in gray:

The design basis flooding (DBF) elevation for the STP 3 & 4 site is determined by considering a number of different flooding scenarios. The potential flooding scenarios applicable and investigated for the site include the following: local probable maximum precipitation (PMP) at the site, potential dam failures, probable maximum flood (PMF) on streams and rivers, probable maximum surge and seiche (PMSS), probable maximum tsunami (PMT), flooding due to ice effects, and flooding caused by channel diversions. In applicable cases the flooding scenarios were investigated in conjunction with other flooding and meteorological events, such as wind-generated waves and tidal levels, as recommended in the guidelines presented in ANSI/ANS 2.8-1992 (Reference 2.4S.2-9). Detailed discussions on each of these flooding

events and how they were estimated are found in Subsections 2.4S.2 through 2.4S.7, and Subsection 2.4S.9. The estimated flood elevations are based on the site plan provided in the COLA Subsection 2.4S.4.

The maximum water level due to a local PMP storm event is estimated and discussed in Subsection 2.4S.2. The maximum water level in the power block area due to a local PMP storm event is estimated to be at elevation 36.6 ft MSL. This level is higher than the ground floor elevation of approximately 35 ft MSL at the Radwaste Buildings for Units 3 and 4, where the postulated accident described in Section 2.4S.13.1.1 occurs. Therefore, a local PMP storm event could potentially pose a flooding risk to a Radwaste Building.

The impacts of postulated dam failures on the STP 3 & 4 safety-related SSCs are discussed in Subsection 2.4S.4. Two aspects of flooding are considered. First, flood elevation at the site is investigated as a result of cascading failure of dams in the Colorado River basin and its tributaries upstream of the site. The resulting water level at the site is 28.6 ft MSL without wind effects, 32.5 ft MSL including coincidental wind set-up, and 34.4 ft including coincidental wind set-up and wave run-up. Second, the flood elevation at the site is investigated due to the failure of the Main Cooling Reservoir (MCR) embankment. A maximum flood elevation of 38.8 ft MSL was determined at the STP 3 & 4 site as a result of the MCR embankment breach. Conservatively, the design basis flood elevation was established at 40.0 ft MSL.

Estimation of the PMF water level on the Colorado River is discussed in Subsection 2.4S.3. The maximum PMF water level for the Colorado River at the STP 3 & 4 site has been determined to be at elevation 26.3 ft MSL. However, including coincidental wind set-up and wave run-up, the water level at the site from the PMF would be slightly lower than about the same as the flood elevation due to cascading failure of dams in the upstream Colorado River basin (34.4 ft MSL). Both flooding scenarios would not could potentially pose a flooding risk to the Radwaste Building.

Flooding from probable maximum surge and seiche as a result of the probable maximum hurricane (PMH) in the Gulf of Mexico is discussed in Subsection 2.4S.5. The maximum water level at the site due to the PMH is estimated to be elevation 31.1 ft MSL. Since this water level is lower than the water level of 32.5 ft for upstream dam failure (with coincidental wind set-up), the resulting maximum water level at the site after factoring in the wave run-up would be lower than 34.4 ft that was predicted for the upstream cascading dam failure event. However, the The water level at the site due to the PMH, including coincidental wind set-up and wave run-up, is not still higher than the entrance elevation to the Radwaste Buildings at STP 3 and STP 4. Therefore, maximum surge and seiche due to the PMH would not could potentially pose a risk of flooding the Radwaste Buildings.

Subsection 2.4S.6 describes estimation of the probable maximum tsunami water level. The maximum water level associated with a PMT at the STP 3 & 4 site is 16.3 ft MSL. Therefore, the PMT would not be a flood risk to the STP 3 & 4 site. As discussed in Subsections 2.4S.7 and 2.4S.9, ice effects and channel diversions, respectively, would not pose a flooding risk to the STP 3 & 4 site.

Of the several flooding mechanisms considered, other than a breach of the MCR embankment, the local PMP storm is the only mechanism having, a cascading failure of upstream dams in the Colorado River basin, the PMF and the PMSS are the four mechanisms that have the potential to flood the Unit 3 and Unit 4 Radwaste Buildings. The local PMP storm potentially could result in release of the greatest concentration of radioactive material to the environment because the flood level from this event would be lower than that from the three other flood mechanisms and, therefore, would provide less dilution if the material were to escape the Radwaste Building.

The local PMP storm eventOther than the MCR breach, each of the four flooding scenarios with the potential to flood the Radwaste Building can be considered a slow-moving event for which advance notice would be available. For this reason, there would be opportunity to initiate operator action to mitigate potential flooding effects. Except during shipment of waste, doors to the Radwaste Building are normally closed to optimize performance of the HVAC system. Upon receiving a flood warning, plant procedures would require securing the doors and implementing other mitigating action such as sandbagging [COM 19.9-3]. Therefore, none of the flooding mechanisms considered presents a credible risk of environmental contamination.